2015

Exploiting Microscale Roughness on Hierarchical Superhydrophobic Copper Surfaces for Enhanced Dropwise Condensation

X. Chen
Purdue University

J A. Weibel
Purdue University, jaweibel@purdue.edu

S V. Garimella
Purdue University, sureshg@purdue.edu

Chen, X.; Weibel, J A.; and Garimella, S V., "Exploiting Microscale Roughness on Hierarchical Superhydrophobic Copper Surfaces for Enhanced Dropwise Condensation" (2015). *CTRC Research Publications.* Paper 247.
http://dx.doi.org/DOI: 10.1002/admi.201400480

DOI: 10.1002/((admi.201400480))
Article type: Communication

Exploiting Microscale Roughness on Hierarchical Superhydrophobic Copper Surfaces for Enhanced Dropwise Condensation

*Xuemei Chen, Justin A. Weibel, and Suresh V. Garimella**

Dr. Xuemei Chen, Prof. Justin A. Weibel, Prof. Suresh V. Garimella

School of Mechanical Engineering and Birck Nanotechnology Center, Purdue University, West Lafayette, Indiana, 47907-2088, USA.
E-mail: sureshg@purdue.edu

Keywords: Superhydrophobic surface, hierarchical roughness, copper substrate, dropwise condensation, droplet departure

Condensation of water vapor is of great interest in thermal management[1] and power generation[2] owing to the improved heat transfer by phase change, and in desalination[3] and dew/fog harvesting[4,5] systems for its ability to extract vapor from carrier gases. Enhancement of the condensation heat and mass transfer processes in these systems could lead to considerable performance gains, economic return, and energy savings. Heterogeneous condensation is dramatically influenced by the physical structure and chemical properties of a surface. Depending on the surface wettability, water vapor can condense on a surface either as a continuous liquid film (filmwise) or as individual droplets (dropwise). It is reported that dropwise condensation can produce heat transfer coefficients that are an order of magnitude higher than in filmwise condensation.[6] To attain this performance, condensed droplets must be rapidly removed from the surface and fresh spaces on the substrate exposed for nucleation; otherwise, accumulated large droplets will act as a thermal barrier and inhibit the heat/mass transfer rate.[7] To promote removal of condensate droplets, the droplet adhesion to the substrate must be minimized. Structured superhydrophobic surfaces[8-12] could offer an ideal

means for enhanced dropwise condensation via improved droplet shedding due to their ability to support spherical water droplets with large contact angle and minimal contact angle hysteresis. However, unlike sessile droplets deposited artificially on such surfaces, droplets formed by condensation grow on all interstitial surfaces of the substrate, from the bottom up. Thus, notionally superhydrophobic surfaces (characterized via sessile droplet deposition) do not necessarily preserve their superhydrophobicity during condensation.[13-15] Previous studies[14,15] have shown that on superhydrophobic surfaces with only microscale roughness, condensate droplets tend to nucleate and grow in the cavities between microstructures, forming sticky droplets in the Wenzel state,[16] which are pinned strongly to the surface at the three-phase contact line. To overcome this limitation, superhydrophobic surfaces with nanoscale[17,18] or hybrid micro/nanoscale[19-24] roughness have been developed that enable the formation of condensate droplets in the Cassie state.

Although nano-structured surfaces can retain their superhydrophobicity and prevent contact-line pinning of droplets during condensation, the development of hybrid surfaces is necessary to promote higher-frequency droplet departure.[18-23] These studies are limited to silicon substrates, however, and are not suitable for scaled-up industrial applications. Therefore, it is highly desirable to develop hybrid surfaces that are compatible with materials commonly employed for heat transfer applications, such as copper. To the best of our knowledge, studies of dropwise condensation on copper substrates have exclusively focused on nano-structured surfaces;[25-27] condensation dynamics on copper surfaces with hierarchical surface structures have not been explored.

In this work, we develop a technique to fabricate hierarchical micro/nano-structured surfaces on copper substrates, and exploit the role of microscale roughness elements to increase the droplet departure frequency during the condensation process. To demonstrate the

effectiveness of such surfaces, the droplet growth rate at the start of condensation and the cumulative droplet self-removal volume for the hierarchical surface are compared to a surface which features only nanostructures.

The hierarchical copper surfaces were fabricated in the Birck Nanotechnology Center at Purdue University. The process flow diagram is shown in Figure S1. The copper substrate (0.5 mm thick) was first cleaned in a diluted HCl solution (volume ratio HCl: deionized (DI) water =1:3) for 2 min, rinsed with DI water, and dried with nitrogen. A photoresist layer was then lithographically patterned onto the copper substrate. This process included spin-coating with hexamethyldisilazane (HMDS) at 3000 rpm for 20 s and photoresist AZ 9260 at 1000 rpm for 30 s. Subsequently, the copper was soft-baked at 100 °C for 15 min and exposed for 78 s at a power of 26 mW/cm^2 under a chrome mask in a mask aligner (MJB-3, Karl Suss). The mask has square arrays of dots (30 μm diameter) at six different pitches (40, 50, 60, 70, 90, and 105 μm). The exposed photoresist layer was developed using AZ 400K in DI water at a dilution ratio of 1:1.5 for 3 min. A photoresist layer with a depth of ~15 μm was produced as a mold for subsequent copper deposition on exposed areas via electroplating. Pulse-electroplating was performed in a custom setup. The electrolyte had three main components: $CuSO_4 \cdot 5H_2O$ (225 g/l), H_2SO_4 (40 g/l), and HCl (50 mg/l). The processing parameters (current density, frequency, and duty cycle) were tuned to achieve dense and uniform copper grains within the exposed areas. Electroplating was performed with a current density of 10 mA/cm^2 at 1 Hz and 50% duty cycle. The total electroplating time to fill the mold was ~2 h. After electroplating, the copper substrate was soaked in acetone for 2 min to dissolve the AZ 9260 photoresist mold and form copper micro-posts on the substrate (Figure S2).

A wet-etching process was performed to form nanostructures on the electroplated micro-structured surface. The copper surface was immersed in an aqueous solution of 2M NaOH and 0.1M $K_2S_2O_8$ for 60 min, rinsed with DI water, and then dried with nitrogen. Hierarchical copper surfaces with micro/nano-structures were thus fabricated (Figure S3); fabrication of hierarchically structured superhydrophobic copper surfaces has not been previously reported. While we do not explore scalability of the method for industrial applications, chemically homogeneous surfaces with patterned micro/nano-scale roughness were created in a controlled manner so as to illustrate the effect of microscale roughness on the condensation dynamics. Scanning electron microscopy (SEM) images of a representative hierarchical surface are shown in **Figure 1**. The low-magnification SEM shows the diameter, height, and edge-to-edge spacing of the micro-posts, which are ~40 μm, ~15 μm, and ~20 μm, respectively (Figure 1a). A close-up image of a single micro-post reveals that the microstructure has a tapered cap, with flower-like nanospheres attached to the underlying nanowire stems (Figure 1b). The diameter of the nanospheres and nanowires are ~2.5 μm and ~150-300 nm, respectively. For comparison purposes, baseline samples were fabricated using subsets of the same procedures to obtain separate single-tier micro-structured and nano-structured surfaces.

To render the surfaces superhydrophobic, all of the samples were silanized through immersion in a 1 mM *n*-hexane solution of 1H,1H,2H,2H-perfluorooctyl-trichlorosilane (PFOS) for 1 hour, followed by heat treatment at ~150 °C on a hotplate for 1 hour. After surface treatment, the static contact angles of the hierarchical surface, nano-structured surface, and micro-structured surface are ~165°, ~160°, and ~150°, respectively.

The chemical compositions and oxidation states of the hierarchical copper samples before and after PFOS silanization were analyzed by X-ray photoelectron spectroscopy (XPS). The XPS results were obtained at the Surface Analysis Facility in the Birck Nanotechnology Center. **Figure 2**a shows the full survey scan spectrum, revealing the photoelectron lines for Cu 3p, Cu 2p, C 1s, O 1s, F 1s, and the Cu LMM and F KLL Auger lines with no detectable impurity elements. To obtain more detailed composition information, high-resolution XPS data were collected for Cu, F, and C elements, as shown in Figure 2b-2d. From assessing the high-resolution scan spectrums of Cu 2p (Figure 2b), there is no significant change before and after surface treatment. Four peaks are detected at 960.6, 953.0, 940.8, and 933.0 eV. The peaks located at 953.0 and 933.0 eV are attributed to the bonding energies of Cu $2p_{1/2}$ and Cu $2p_{3/2}$, respectively, and the two satellite peaks at 960.8 and 940.8 eV are shake-up lines of Cu(II) oxide.[28,29] Because each peak at 950.0 eV and 933.0 eV can be fitted to only one Gaussian (70%)–Lorentzian (30%) peak shape, the Cu 2p lines correspond to only one oxidation state, indicating that the samples contain only CuO.[29,30] From Figure 2c and 2d, we can see that after being silanized, a strong F 1s peak at 687.9 eV and two new C 1s peaks at 290.4 and 292.8 eV appear, which can be assigned to $–CF_2$ and $–CF_3$ groups, respectively.[31] This demonstrates that PFOS has been self-assembled or absorbed onto the surface of the hierarchical structure.

The condensation experiments were carried out in an environment at an ambient temperature of ~22 °C and relative humidity of ~40% (absolute humidity of ~7.76 g/m^3). The samples were mounted onto a vertically oriented thermoelectric cooling stage (CP-031, TE Technology, Inc.) using carbon adhesive tape to provide thermal contact. The temperature of the cooling stage was reduced from the ambient temperature to 0 °C. The condensation

process was recorded at 6 fps by a CCD camera (EO-5023M, Edmund Optics) equipped with a wide-range zoom lens (VH-Z100R, Keyence); in-line illumination was provided with a 300 W Xe arc lamp (TITAN 300, Sunoptic Technologies). In order to observe the condensation process from the side, the cooling stage was reconfigured to a horizontal orientation, and the samples were visualized by a high-speed camera (FASTCAM 1024 PCI, Photron) at 3000 fps.

We first study the time evolution of condensation dynamics on the hierarchical surface (**Figure 3**). The condensate droplets preferentially nucleate along the corners at the base of the micro-posts where they intersect with the substrate (see the encircled droplet in Figure 3a); in this configuration the liquid-vapor interfacial area of the droplet is minimized.[32] We observe that it is not necessary to create smooth hydrophobic spots at the base of micro-structures[19-21] in order to promote condensate droplet nucleation and departure. To confirm this behavior at a higher resolution, we conducted additional condensation experiments on the hierarchical copper surfaces using environmental scanning electron microscope (ESEM, FEI Quanta 3D, ~6 torr, ~3 °C stage) (Figure S4). As condensation proceeds, the contact line of the condensate droplet remains pinned at the pillar base corners, and the droplet appears to grow in a constant contact line mode. Similar droplet nucleation behavior is observed on the surface with only micro-structures (Figure S5a). In contrast, random heterogeneous nucleation was observed on the nano-structured surface (Figure S5b). This clearly demonstrates that microscale roughness strongly influences the location of droplet nucleation.

Once we identified the role of microscale roughness in controlling the droplet nucleation and growth process, we further investigated the condensate droplet departure dynamics on the hierarchical surface as well as baseline samples. As the condensation progresses on the hierarchical surface, the condensate droplets rapidly grow and reach a metastable spherical shape. When adjacent metastable droplets coalesce, sufficient surface energy is released to

overcome the adhesion of the droplet to the surface, resulting in droplet departure from the surface.[24,33,34] This departure can result either in the jumping or random sweeping of mobile droplets off the surface (see the droplets enclosed by the dashed lines in Figure 3b). As a result, many fresh areas on the substrate are exposed and can contribute to the cyclical process of nucleation, coalescence, and departure; a high frequency of surface refreshing, which shifts the distribution of droplets on the surface to smaller sizes, will lead to high heat transfer coefficients in dropwise condensation.[35] For the hierarchical surfaces in particular, a majority of coalescence-induced droplet departure events take place in between adjacent micro-posts and multiple participating droplets are involved in each coalescence event (Figure 3b). In addition to droplet jumping by coalescence of condensate droplets (Figure 3c), it is interesting to note that out-of-plane jumping motion can also be triggered by falling droplets coalescing with other droplets on the surface (Figure 3d). Although the surface is oriented in the vertical direction with respect to gravity, the influence of gravity on droplet departure is negligible, as the average diameter of departing droplets (~30 μm) is two orders of magnitude smaller than the capillary length scale (~2 mm).[36] This departure size is in close agreement with previous experimental observations and theoretical predictions.[37-39] From the set of hierarchical surfaces investigated (Figure S3), droplets departed most frequently from the surface with an edge-to-edge pillar spacing of ~20 μm.

Condensation behavior over a longer period is compared between the hierarchical and baseline samples. As expected, condensate droplets stay in the Wenzel state on the surface with only micro-posts, and the accumulated water transitions to a filmwise condensation mode over time (Figure S5a, Movie 1); liquid removal in the form of a film from the surface then relies on gravity. The nano-structured surface exhibits dropwise condensation behavior;

however, the droplet departure frequency is much lower relative to that on the hierarchical surface (Movie 2 and 3). Hence, after ~1 h of condensation, the droplet surface coverage on the surface with only nanoscale roughness is larger compared to the hierarchical surface (Figure S5b and S5c).

To quantitatively illustrate the benefit of incorporating microscale roughness along with nanostructuring, the cumulative droplet departure volume is calculated by comparing sequential images taken at 20 sec intervals. As shown in **Figure 4**a, the cumulative departure volume over time is markedly higher for the hierarchical surface as compared to the nano-structured surface. After 30 min of condensation, an increase of over 300% in the cumulative droplet departure volume is achieved on the hierarchical surface within the approximately 495 μm × 370 μm field of view. The corresponding time evolution of surface coverage by condensate droplets is illustrated in Figure 4b. While individual droplet departure events cause fluctuations in this surface areas coverage measurement, the hierarchical and nano-structured surfaces maintain a constant average surface coverage, indicative of continuous dropwise condensation, after the first ~300 s. Both surfaces sustain this behavior over long durations; however, during this period of sustained dropwise condensation, the hierarchical surface has a smaller average surface coverage (~0.39±0.03) than the nano-structured surface (~0.43±0.015). This further demonstrates the superiority of the hierarchical surface for promoting droplet departure.

This enhanced droplet departure performance on the hierarchical surface is attributed to several growth and departure mechanisms that the unique microscale roughness features enable and exploit. First, at the start of condensation, water droplets primarily nucleate at the bases of the micro-posts (as exemplified by the encircled droplet in Figure 3a), and grow

rapidly while the contact line is confined at the base corner. The time evolution of the average droplet radius is plotted in Figure 4c. At the very beginning of condensation, before droplet coalescence occurs, the exponent of the growth power law ($r \sim t^{\alpha}$, where r is the droplet radius) for an isolated droplet on the hierarchical surface is ~0.48±0.03, which is ~40% higher than that on the nano-structured surface (~0.34±0.03). The increased α for the hierarchical surface, as compared to the well-known one-third power law ($\alpha \approx 1/3$),[40] may be attributed to the effect of the microstructure corners, which serve as favorable heterogeneous nucleation sites, and promote condensation on the droplet.[19,41] Also, the micro-posts provide a constant edge-to-edge spacing of ~20 μm, and a majority of the departing droplets coalesce in this space (Figure 3b). Combined with a faster growth rate for individual droplets, this ordered droplet nucleation process increases the probability for coalescence of multiple droplets in the interstices between micro-posts (in comparison to the random coalescence events that occur on the more homogeneous nano-structured surface). Second, the presence of nanoscale roughness on the hierarchical surface increases the local condensate droplet contact angle θ,[18,42,43] which reduces the work of adhesion (W_{ad}) of the droplet to the surface ($W_{ad} = \sigma_{lv}(1+\cos\theta)$ where σ_{lv} is the liquid/vapor interfacial tension);[24] the tapered nature of the micro-post surfaces reduces the solid-liquid contact area, which further decreases the contact angle hysteresis.[19] Thus, the synergistic cooperation between the micro and nanoscale roughnesses on the hierarchical surface eases condensate droplet departure from the surface. Lastly, when the condensate droplet grows in a position resting on the inclined posts (Figure 4d), the Laplace pressure is expressed as:[27,44,45] $\Delta p = p - p_0 = -\dfrac{\sigma_{lv}\cos(\theta-\alpha)}{R_0 + h\tan\alpha}$,

where θ is Young's contact angle for the droplet on the surface, α is the inclination angle,

R_0 is half the distance between the base edges of two adjacent inclined walls, p is the pressure on the liquid side of the meniscus, p_0 is the atmospheric pressure, and h is the water height, which is dependent on the hydrostatic pressure of water on top of the structured surface. On the hierarchical surface, the Laplace pressure is amplified because the contact angle θ is increased as a result of the nanoscale secondary structure such that the water meniscus moves away from the bottom of the hierarchical structures. The increased Laplace pressure thereby acts as a driving force for the upward condensate droplet movement.

In summary, we developed a technique to fabricate hierarchical micro/nano-structured superhydrophobic surfaces on copper substrates. The microscale surface features are arranged so as to control the droplet nucleation and growth in a manner that exploits the mechanisms of droplet departure from the surface. In addition, the combined micro/nanoscale roughness is used to tailor the surface wetting characteristics as desired. Though the surfaces are chemically homogeneous, without heterogeneous nucleation sites (such as hydrophilic/hydrophobic spots), synergistic cooperation between the primary surface design features jointly contributes to the enhanced droplet nucleation, growth, and departure. Such enhanced condensation performance on hierarchical copper surfaces offers an avenue for developing higher-performance thermal management and psychrometric systems.

Supporting Information
Supporting Information is available from the Wiley Online Library or from the author.

Acknowledgements
We gratefully acknowledge financial support provided by the Cooling Technologies Research Center, a National Science Foundation Industry/University Cooperative Research Center at Purdue University. We thank Ravi S. Patel for configuring the visualization system used for the condensation studies.

Received: ((will be filled in by the editorial staff))
Revised: ((will be filled in by the editorial staff))
Published online: ((will be filled in by the editorial staff))

References

[1] J. B. Boreyko, C.-H. Chen, *Int. J. Heat Mass Transfer* **2013**, *61*, 409.

[2] J. M. Beér, *Prog. Energy Combust. Sci.* **2007**, *33*, 107.

[3] T. Humplik, J. Lee, S. C. O'Hern, B. A. Fellman, M. A. Baig, S. F. Hassan, M. A. Atieh, F. Rahman, T. Laoui, R. Karnik, *Nanotechnology* **2011**, *22*, 292001.

[4] A. Lee, M.-W. Moon, H. Lim, W.-D. Kim, H.-Y. Kim, *Langmuir* **2012**, *28*, 10183.

[5] H. G. Andrews, E. A. Eccles, W. C. E. Schofield, J. P. S. Badyal, *Langmuir* **2011**, *27*, 3798.

[6] E. Schmidt, W. Schurig, W. Sellschopp, *Tech. Mech. Thermondyn.* **1930**, *1*, 53.

[7] N. Miljkovic, R. Enright, E. N. Wang, *ACS Nano* **2012**, *6*, 1776.

[8] A. Lafuma, D. Quéré, *Nat. Mater.* **2003**, *2*, 457.

[9] S. Dash, M. T. Alt, S. V. Garimella, *Langmuir* **2012**, *28*, 9606.

[10] Z. Wang, N. Koratkar, L. Ci, P. M. Ajayan, *Appl. Phys. Lett.* **2007**, *90*, 143117.

[11] X. Chen, R. Ma, J. Li, C. Hao, W. Guo, B. L. Luk, S. C. Li, S. Yao, Z. Wang, *Phys. Rev. Lett.* **2012**, *109*, 116101.

[12] H. Teisala, M. Tuominen, J. Kuusipalo, *Adv. Mater. Interfaces* **2014**, *1*, 1300026.

[13] T. Furuta, M. Sakai, T. Isobe, A. Nakajima, *Langmuir* **2010**, *26*, 13305.

[14] R. D. Narhe, D. A. Beysens, *Langmuir* **2007**, *23*, 6486.

[15] K. A. Wier, T. J. McCarthy, *Langmuir* **2006**, *22*, 2433.

[16] R. N. Wenzel, *Ind. Eng. Chem.* **1936**, *28*, 988.

[17] C. Dietz, K. Rykaczewski, A. G. Fedorov, Y. Joshi, *Appl. Phys. Lett.* **2010**, *97*, 033104.

[18] K. Rykaczewski, W. A. Osborn, J. Chinn, M. L. Walker, J. H. J. Scott, W. Jones, C. Hao, S. Yao, Z. Wang, *Soft Matter* **2012**, *8*, 8786.

[19] X. Chen, J. Wu, R. Ma, M. Hua, N. Koratkar, S. Yao, Z. Wang, *Adv. Funct. Mater.* **2011**, *21*, 4617.

[20] X. Chen, R. Ma, H. Zhou, X. Zhou, L. Che, S. Yao, Z. Wang, *Sci. Rep.* **2013**, *3*, 2515.

[21] K. Rykaczewski, A. T. Paxson, S. Anand, X. Chen, Z. Wang, K. K. Varanasi, *Langmuir* **2012**, *29*, 881.

[22] T. Liu, W. Sun, X. Sun, H. Ai, *Langmuir* **2010**, *26*, 14835.

[23] J. Cheng, A. Vandadi, C.-L. Chen, *Appl. Phys. Lett.* **2012**, *101*, 131909.

[24] M. He, X. Zhou, X. Zeng, D. Cui, Q. Zhang, J. Chen, H. Li, J. Wang, Z. Cao, Y. Song, L. Jiang, *Soft Matter* **2012**, *8*, 6680.

[25] D. Torresin, M. K. Tiwari, D. Del Col, D. Poulikakos, *Langmuir* **2012**, *29*, 840.

[26] N. Miljkovic, R. Enright, Y. Nam, K. Lopez, N. Dou, J. Sack, E. N. Wang, *Nano Lett.* **2012**, *13*, 179.

[27] J. Feng, Y. Pang, Z. Qin, R. Ma, S. Yao, *ACS Appl. Mater. Interfaces* **2012**, *4*, 6618.

[28] J. F. Moulder, W. F. Stickle, P. E. Sobol, K. D. Bomben, *Handbook of X-Ray Photoelectron Spectroscopy*, Perkin-Elmer Corporation, Eden Prairie, Minnesota, USA **1992**.

[29] M. C. Biesinger, L. W. M. Lau, A. R. Gerson, R. S. C. Smart, *Appl. Surf. Sci.* **2010**, *257*, 887.

[30] S.-M. Lee, K.-S. Kim, E. Pippel, S. Kim, J.-H. Kim, H.-J. Lee, *J. Phys. Chem. C* **2012**, *116*, 2781.

[31] Z. He, M. Ma, X. Lan, F. Chen, K. Wang, H. Deng, Q. Zhang, Q. Fu, *Soft Matter* **2011**, *7*, 6435.

[32] C. Dorrer, J. Rühe, *Langmuir* **2007**, *23*, 3820.

[33] C. Lv, P. Hao, Z. Yao, Y. Song, X. Zhang, F. He, *Appl. Phys. Lett.* **2013**, *103*, 021601.

[34] J. Tian, J. Zhu, H.-Y. Guo, J. Li, X.-Q. Feng, X. Gao, *J. Phys. Chem. Lett.* **2014**, *5*, 2084.

[35] C. Graham, P. Griffith, *Int. J. Heat Mass Transfer* **1973**, *16*, 337.

[36] L. R. Glicksman, A. W. Hunt Jr, *Int. J. Heat Mass Transfer* **1972**, *15*, 2251.

[37] J. B. Boreyko, C.-H. Chen, *Phys. Rev. Lett.* **2009**, *103*, 184501.

[38] F.-C. Wang, F. Yang, Y.-P. Zhao, *Appl. Phys. Lett.* **2011**, *98*, 053112.

[39] Y. Nam, H. Kim, S. Shin, *Appl. Phys. Lett.* **2013**, *103*, 161601.

[40] J. L. Viovy, D. Beysens, C. M. Knobler, *Phys. Rev. A* **1988**, *37*, 4965.

[41] K. K. Varanasi, M. Hsu, N. Bhate, W. Yang, T. Deng, *Appl. Phys. Lett.* **2009**, *95*, 094101.

[42] K. K. S. Lau, J. Bico, K. B. K. Teo, M. Chhowalla, G. A. J. Amaratunga, W. I. Milne, G. H. McKinley, K. K. Gleason, *Nano Lett.* **2003**, *3*, 1701.

[43] C. Dorrer, J. Rühe, *Adv. Mater.* **2008**, *20*, 159.

[44] Y. Xiu, L. Zhu, D. W. Hess, C. P. Wong, *Nano Lett.* **2007**, *7*, 3388.

[45] M. Gong, Z. Yang, X. Xu, D. Jasion, S. Mou, H. Zhang, Y. Long, S. Ren, *J. Mater. Chem. A* **2014**, *2*, 6180.

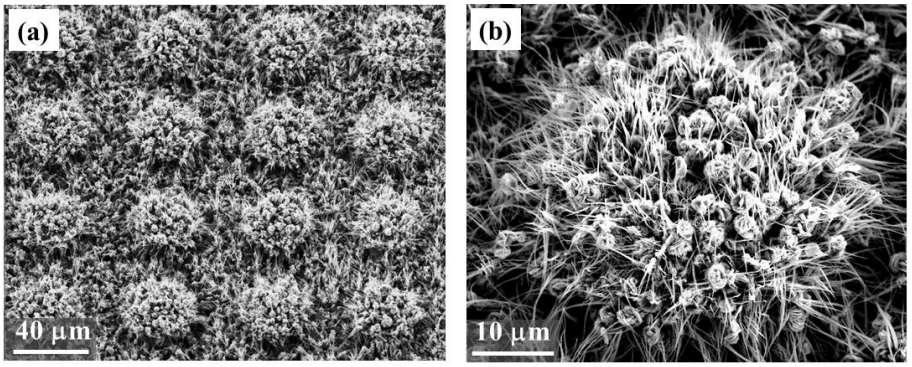

Figure 1. (a) SEM image of the hierarchical micro/nano-structured copper surface having a square array of tapered micro-posts (shown before silanization). (b) A close-up SEM image showing an individual micro-post decorated with nanowire stems supporting flower-like nanospheres.

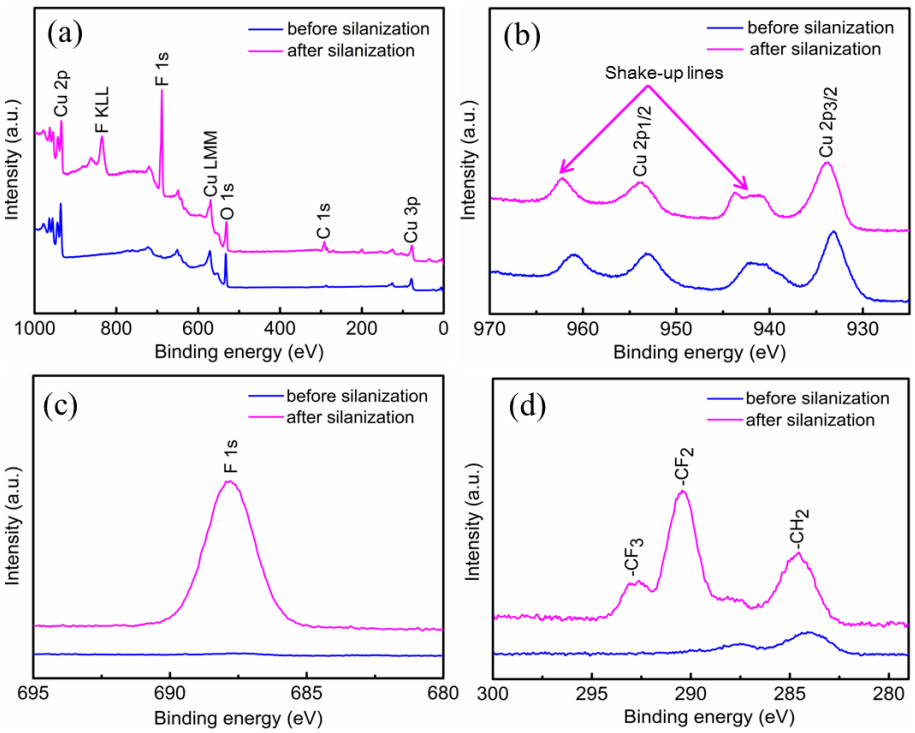

Figure 2. XPS spectra of the hierarchical surfaces before and after PFOS silanization: (a) full spectrum and (b-d) core-level spectra of Cu 2p, F 1s, and C 1s, respectively.

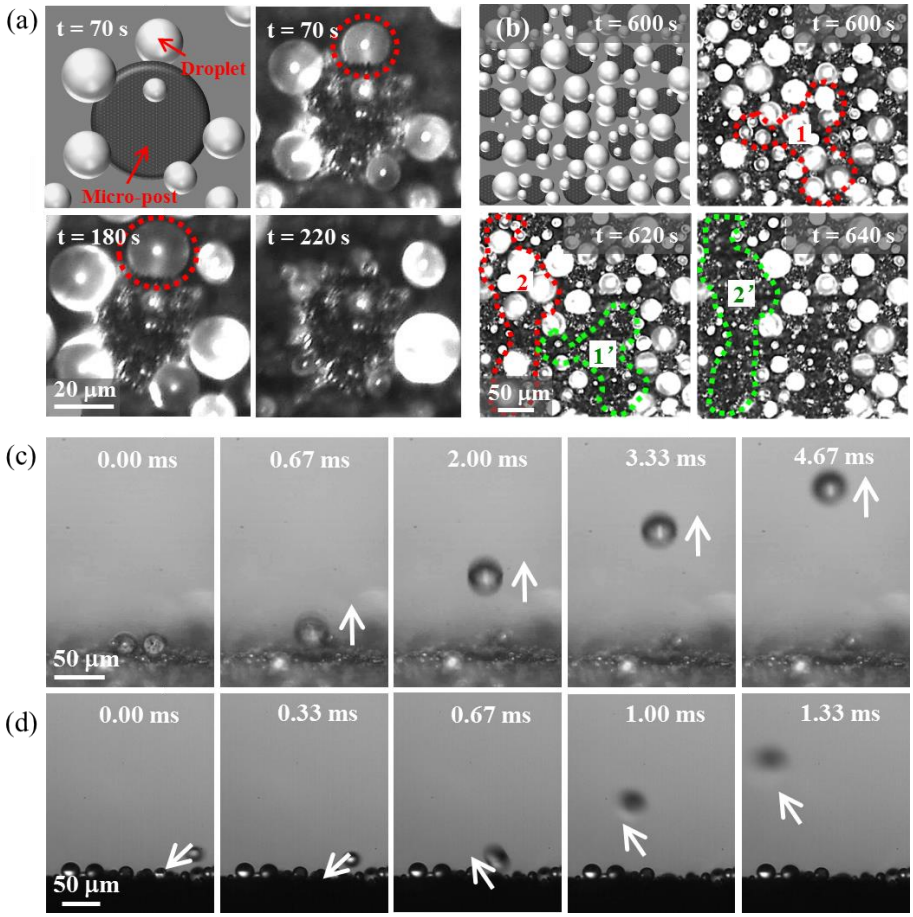

Figure 3. (a) Selected photographs showing the nucleation and growth of a droplet on the hierarchical surface. The encircled condensate droplet forms at a corner along the base of the micro-post; the droplet grows in size with a constant contact line and attains a near-spherical shape (70~180 s), and then disappears as a result of coalescence with neighboring droplets (220 s). (b) Selected photographs showing the droplet departure dynamics on the hierarchical copper surface. The dashed lines indicate two groups of spherical condensate droplets (1 and 2) which, upon coalescence, experience out-of-plane jumping or sweeping that exposes a fresh space on the substrate for new droplet formation (1' and 2'). The upper left corner images of (a) and (b) are schematic drawings that illustrate the location of droplets and posts. (c) Selected high-speed camera images showing droplet jumping induced by the coalescence of two sessile condensate droplets, and (d) droplet jumping triggered by a falling droplet. The white arrows show the direction of the moving droplets.

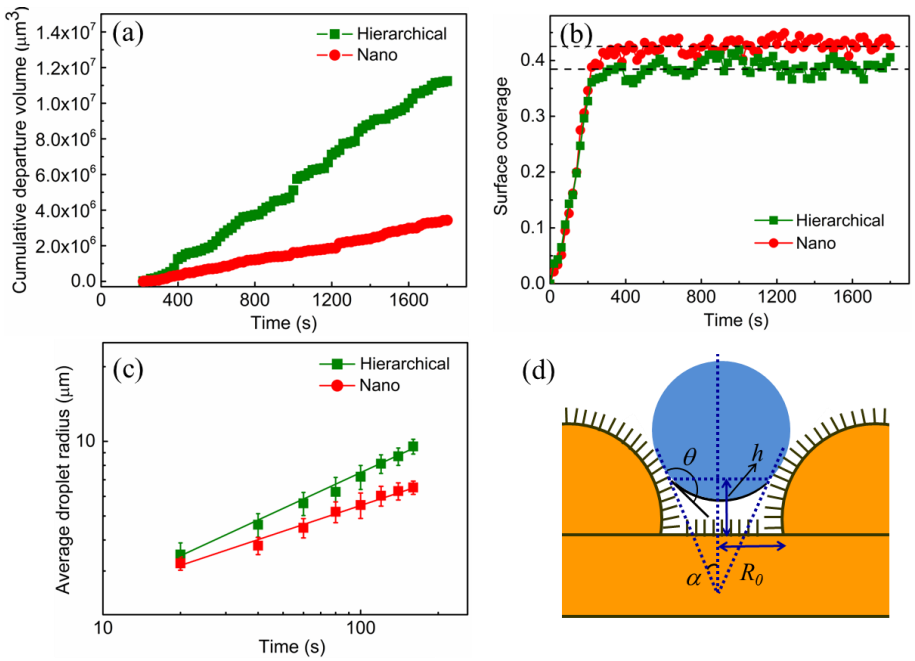

Figure 4. Quantitative analysis of the condensation processes on the hierarchical and nanostructured surfaces: (a) droplet cumulative departure volume over 30 min; (b) time evolution of droplet surface coverage; (c) comparison of average droplet radius as a function of time from the beginning of condensation (error bars are obtained from measuring multiple droplets at different locations across the corresponding samples); and (d) schematic drawing showing condensate droplet sitting on the inclined planes of neighboring posts on the hierarchical surface.

The table of contents:

Hierarchical micro/nano-structured superhydrophobic surfaces are developed to control the nucleation, growth, and departure of condensate droplets on copper substrates. The microscale roughness elements on the hierarchical surface yield a 40% higher droplet growth rate and a 300% increase in cumulative droplet departure volume as compared to superhydrophobic surfaces with nanostructures alone.

Keywords: Superhydrophobic surface, dropwise condensation, hierarchical roughness, copper substrate

Xuemei Chen, Justin A. Weibel, Suresh V. Garimella

Exploiting Microscale Roughness on Hierarchical Superhydrophobic Copper Surfaces for Enhanced Dropwise Condensation